Lattice QCD Constraints on Pion Electroproduction off a Nucleon

Zhan-Wei Liu

School of Physical Science and Technology, Lanzhou University, China

Light Hadron Workshop in 2026, Shangqiu

15/5/2026

Electron nucleon scattering process are important in particle physics!

- At large energy scales:
  - Deep inelastic scattering reveals the parton structure of nucleons.
  - Perturbative QCD is very successful.
- At low energy scales:
  - Electroproduction off the nucleon can help constrain the nuclear force.
  - Non-perturbative dynamics of QCD is still developing.

We will report our study for the pion electroproduction off a nucleon at low energies

$$e + N \rightarrow e + N + \pi.$$

In this process, the πN Rescattering Effects cannot be neglected.

1. Constraints from the πN scattering data

$N^*(1535)$ with πN Scattering

$N^*(1535)$ is the lowest resonance with $I(J^P) = \frac{1}{2}(\frac{1}{2}^-)$.

- One needs to consider the interactions

  among the bare baryon N_0^*, πN channel, and ηN channel.

$$G^2_{\pi N;N_0^*}(k) = \frac{3g^2_{\pi N;N_0^*}}{4\pi^2 f^2}\omega_\pi(k)$$

$$V^S_{\pi N,\pi N}(k,k') = \frac{3g^S_{\pi N}}{4\pi^2 f^2}\frac{m_\pi + \omega_\pi(k)}{\omega_\pi(k)}\frac{m_\pi + \omega_\pi(k')}{\omega_\pi(k')}$$

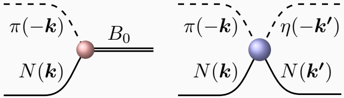

- Phase shifts and inelasticities

  are obtained by solving Bethe-Salpeter equation with the interactions.

$$T_{\alpha,\beta}(k,k';E) = V_{\alpha,\beta}(k,k') + \sum_\gamma \int q^2 dq V_{\alpha,\gamma}(k,q)\frac{1}{E - \sqrt{m^2_{\gamma_1} + q^2} - \sqrt{m^2_{\gamma_2} + q^2} + i\epsilon}T_{\gamma,\beta}(q,k';E)$$

$N^*(1535)$ with πN scattering at infinite volume

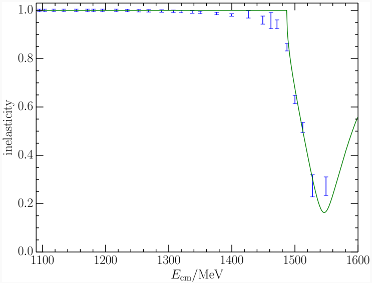

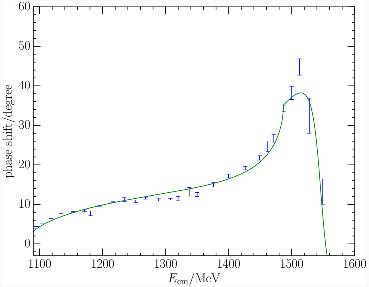

πN Scattering with $I(J^P) = \frac{1}{2}(\frac{1}{2}^-)$.

Our Pole: $1531 \pm 29 - i\ 88 \pm 2$ MeV.

Particle Data Group: $1510 \pm 20 - i\ 85 \pm 40$ MeV.

Z. W. Liu, W. Kamleh, D. B. Leinweber, F. M. Stokes, A. W. Thomas and J. J. Wu, Phys. Rev. Lett. 116 (2016) no.8, 082004

2. Constraints from the lattice QCD N^* mass spectra

Scattering Data vs. Lattice QCD data

Usually masses and widths of resonances are extracted from the scattering experiments

- closely related to the channel interaction;
- tangled with different quantum numbers.

Nowadays Lattice QCD provides abundant of finite-volume mass spectra.

- starting from the first principle of QCD;
- easier to extract results for one quantum number independently;
- different physics from the infinite volume.

Scattering Data and Lattice QCD data are both important.

- Lüscher formalism
  - model independent:
    the hadron interactions and structures are not needed;
  - single-channel efficient:

$$\text{lattice QCD energies} \overset{\text{Lüscher formalism}}{\Longrightarrow} \text{scattering phaseshifts} \Longrightarrow \text{masses and widths.}$$

- Hamiltonian Effective Field Theory (HEFT)
  - multi-channel friendly;
  - Scattering Data and Lattice QCD data can be simultaneously analyzed with HEFT

$$\left.\begin{array}{l}\text{scattering data} \\ \\ \text{lattice QCD data}\end{array}\right\} \overset{\text{HEFT}}{\Longrightarrow} \text{effective potentials} \Longrightarrow \text{masses and widths;}$$

    Hadron interactions and structures can be studied.

- Other approaches

Discretization in finite volume

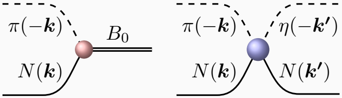

$$\tilde{G}_i(k_n) = \sqrt{\frac{C_3(n)}{4\pi}}(\frac{2\pi}{L})^{3/2} G_i(k_n),$$

$$\tilde{V}^S_{i,j}(k_n, k_m) = \frac{\sqrt{C_3(n)C_3(m)}}{4\pi}(\frac{2\pi}{L})^3 V^S_{i,j}(k_n, k_m).$$

$C_3(n)$ represents the number of summing the squares of three integers to equal n.

With the eigen-solution of the discretized Hamiltonian, one can obtain the mass spectrum and the components.

$$H_0 = \text{diag}\{m^0_{N_1}, \omega_{\pi N}(k_0),\ \omega_{\eta N}(k_0), \omega_{\pi N}(k_1),\ \omega_{\eta N}(k_1), ...\},$$

$$H_I = \begin{pmatrix} 0 & \tilde{G}_{\pi N}(k_0) & \tilde{G}_{\eta N}(k_0) & \tilde{G}_{\pi N}(k_1) & \tilde{G}_{\eta N}(k_1) & \cdots \\ \tilde{G}_{\pi N}(k_0) & \tilde{V}^S_{\pi N,\pi N}(k_0, k_0) & 0 & \tilde{V}^S_{\pi N,\pi N}(k_0, k_1) & 0 & \cdots \\ \tilde{G}_{\eta N}(k_0) & 0 & 0 & 0 & 0 & \cdots \\ \tilde{G}_{\pi N}(k_1) & \tilde{V}^S_{\pi N,\pi N}(k_1, k_0) & 0 & \tilde{V}^S_{\pi N,\pi N}(k_1, k_1) & 0 & \cdots \\ \tilde{G}_{\eta N}(k_1) & 0 & 0 & 0 & 0 & \cdots \\ \vdots & \vdots & \vdots & \vdots & \vdots & \ddots \end{pmatrix},$$

Spectra at Finite Volumes

3 sets of lattice QCD data at different pion masses and finite volumes

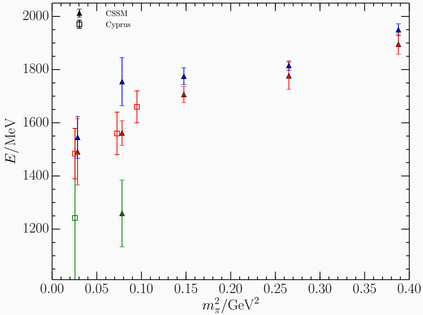

$L \approx 3$ fm

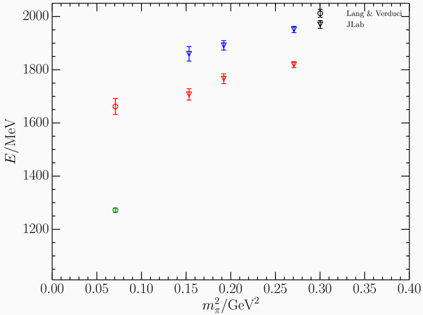

$L \approx 2$ fm

N^* Spectra with $I(J^P) = \frac{1}{2}(\frac{1}{2}^-)$ at finite volumes

Spectra at Finite Volumes

3 sets of lattice QCD data at different pion masses and finite volumes

Non-interacting energies of the two-particle channels

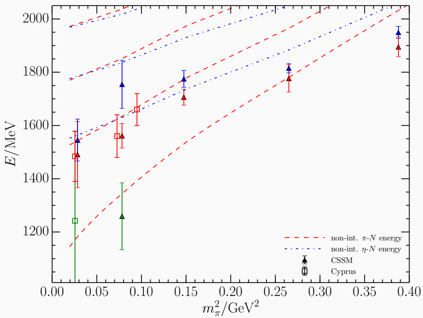

$L \approx 3$ fm

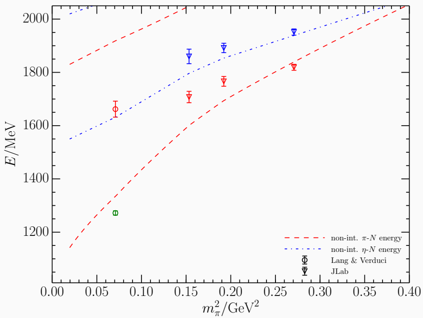

$L \approx 2$ fm

N^* Spectra with $I(J^P) = \frac{1}{2}(\frac{1}{2}^-)$ at finite volumes

Spectra at Finite Volumes

3 sets of lattice QCD data at different pion masses and finite volumes

Non-interacting energies of the two-particle channels

Eigenenergies of Hamiltonian effective field theory

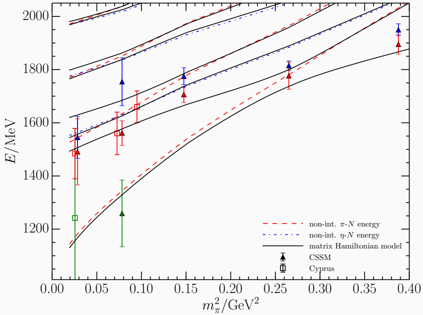

$L \approx 3$ fm

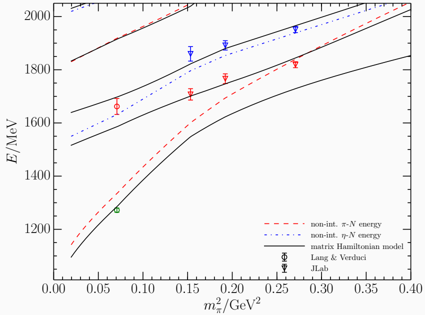

$L \approx 2$ fm

N^* Spectra with $I(J^P) = \frac{1}{2}(\frac{1}{2}^-)$ at finite volumes

Spectra at Finite Volumes

3 sets of lattice QCD data at different pion masses and finite volumes

Eigenenergies of Hamiltonian effective field theory

Coloured lines indicating most probable states observed in LQCD

We not only provide the mass but also analyze why some states are observed on the lattice

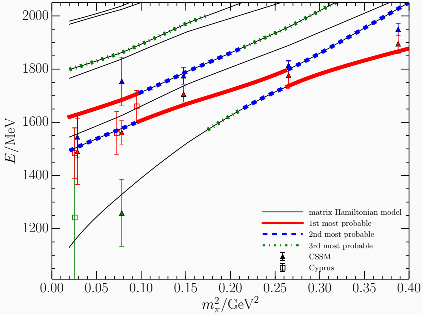

$L \approx 3$ fm

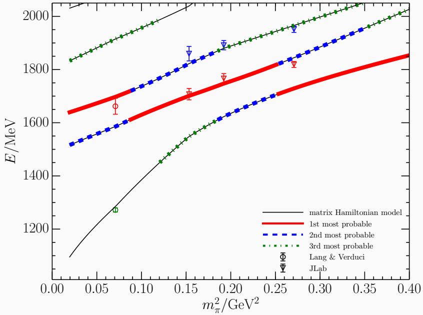

$L \approx 2$ fm

N^* Spectra with $I(J^P) = \frac{1}{2}(\frac{1}{2}^-)$ at finite volumes

Explicitly including $N^*(1650)$ as well as $N^*(1535)$

In Phys. Rev. D 108 (2023) 9, 094519, we consider

- two bare baryon states N_1 and N_2;
- πN, ηN, and $K\Lambda$;
- more experimental data with larger energies (1.60, 1.75) GeV.

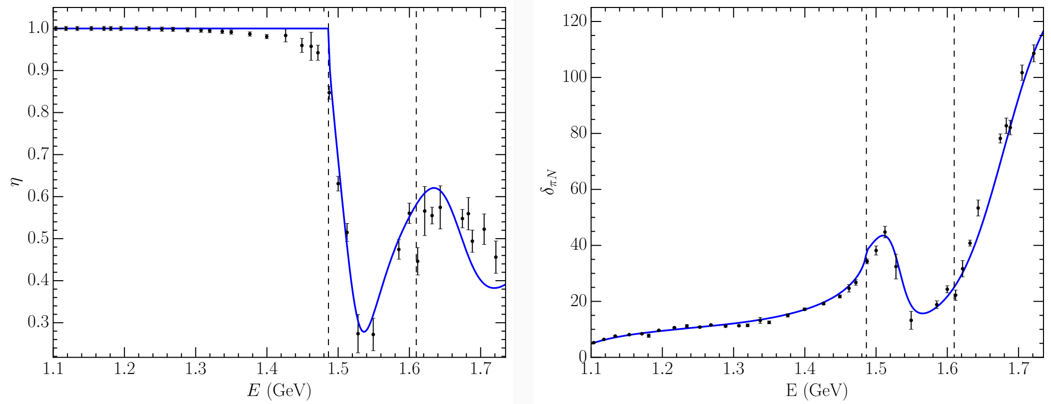

Pole positions for $N^*(1535)$ and $N^*(1650)$

In the Particle Data Group (PDG) tables, the poles for the two low-lying odd-parity nucleon resonances are given as

$$E_{N^*(1535)} = 1510 \pm 10 - (65 \pm 10)i \text{ MeV},$$
$$E_{N^*(1650)} = 1655 \pm 15 - (67 \pm 18)i \text{ MeV}.$$

Using HEFT, two poles for $N^*(1535)$ and $N^*(1650)$ in the second Riemann sheet are found at energies

$$E_1 = 1500 - 50i \text{ MeV},$$
$$E_2 = 1658 - 56i \text{ MeV}.$$

Our results are in excellent agreement with the PDG pole positions.

Finite-volume spectrum

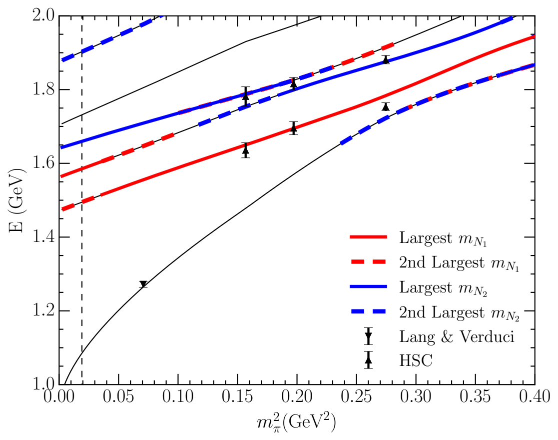

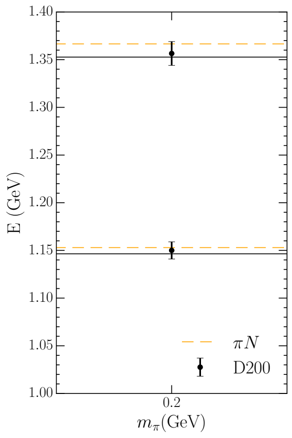

$L \sim 2$ fm

$L \sim 4$ fm

C. D. Abell, D. B. Leinweber, Z.-W. Liu, A. W. Thomas, J.-J. Wu, PRD 108 (2023) 9,094519

We develop Hamiltonian effective field theory to study other resonances.

Based on scattering data and lattice QCD data, we have developed Hamiltonian effective field theory to study other baryon resonances.

We develop Hamiltonian effective field theory to study other resonances.

Based on scattering data and lattice QCD data, we have developed Hamiltonian effective field theory to study other baryon resonances. For example, $N(938)$ & $N(1440)$ in $N(1/2^+)$ family:

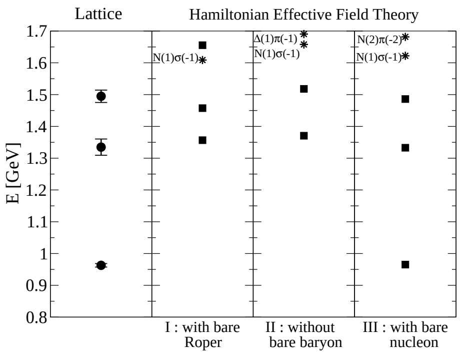

- All 3 lowest energy levels of HEFT were observed by the latter lattice QCD simulations.
- They support our Scenario III: the $N(1440)$ are mainly dynamically generated by the couplings of πN, $\pi\Delta$, etc.

An original figure from later lattice QCD work (Lang et. al. PRD95 (2017) no.1, 014510)

We develop Hamiltonian effective field theory to study other resonances.

Based on scattering data and lattice QCD data, we have developed Hamiltonian effective field theory to study other baryon resonances. For example, $\Lambda(1405)$ & $\Lambda(1670)$ in $\Lambda(1/2^-)$ family:

$L \sim 3$ fm

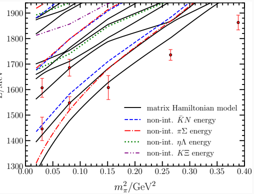

without

a bare baryon

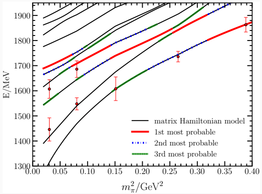

with

a bare baryon

- $\Lambda(1405)$ is mainly the $\bar{K}N$ molecule, and the triquark core $uds(1P)$ goes into $\Lambda(1670)$.

J.-J. Liu, Z.-W. Liu, K. Chen, D. Guo, D. B. Leinweber, X. Liu, A. W. Thomas, Phys. Rev. D 109 (2024) 5, 054025.

We develop Hamiltonian effective field theory to study other resonances.

Based on scattering data and lattice QCD data, we have developed Hamiltonian effective field theory to study other baryon resonances. For example, $\Lambda(1405)$ & $\Lambda(1670)$ in $\Lambda(1/2^-)$ family:

$L \sim 4$ fm

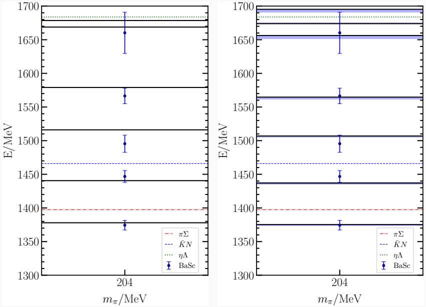

without a bare baryon | with a bare baryon

- $\Lambda(1405)$ is mainly the $\bar{K}N$ molecule, and the triquark core $uds(1P)$ goes into $\Lambda(1670)$.
- The BaSc lattice collaboration observed all HEFT states with multiquark interpolating operators;
- The right HEFT results with bare Λ fit the lattice simulations better;

J.-J. Liu, Z.-W. Liu, K. Chen, D. Guo, D. B. Leinweber, X. Liu, A. W. Thomas, Phys. Rev. D 109 (2024) 5, 054025.

We develop Hamiltonian effective field theory to study other resonances.

Based on scattering data and lattice QCD data, we have developed Hamiltonian effective field theory to study other baryon resonances. For example, in $\Sigma(1/2^-)$ family:

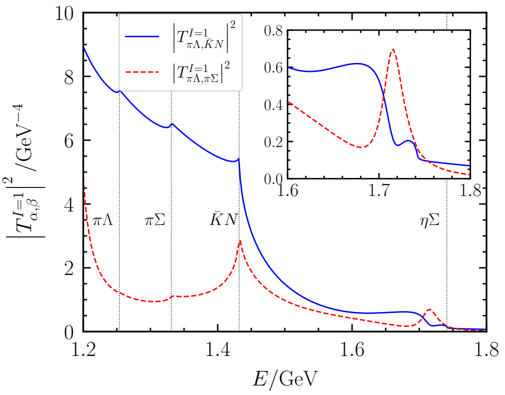

For $\left|T^{I=1}_{\pi\Lambda,\bar{K}N}\right|^2$ (blue lines)

- a wide peak around 1.68 GeV
- a narrow one around 1.73 GeV

corresponding to the two poles found on the (uuupp) sheet.

A clear cusp-like structures at the $\bar{K}N$ threshold in the $\pi\Sigma \to \pi\Lambda$ scattering.

Z.-L. Ma, Z.-W. Liu, J.-J. Liu, Phys. Rev. D 113 (2026) 1, 014037.

3. Constraints from the $\gamma N \to \pi N$ scattering

Pion Photoproduction off Nucleon with Hamiltonian EFT

- The essential part of pion electroproduction process $e + N \to e + \pi + N$ is

$$\gamma^*(q) + N(p) \to \pi(k) + N(p')$$

- This process can be mainly divided into two parts

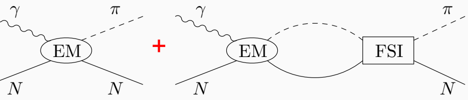

$$\mathcal{M}(\gamma N \to \pi N) \sim \mathcal{M}^{\text{EM}}(\gamma N \to \pi N) + \mathcal{M}^{\text{EM}}(\gamma N \to \pi N) \otimes \mathcal{M}^{\text{FSI}}(\pi N \to \pi N) + \mathcal{M}^{\text{EM}}(\gamma N \to \eta N) \otimes \mathcal{M}^{\text{FSI}}(\eta N \to \pi N)$$

- The final-state-interaction parts have been carefully studied through analyzing
  - $\pi N \to \pi N$
  - lattice QCD spectrum of N^*
- The electromagnetic potential parts are obtained by some tree diagrams.

Electromagnetic Multipoles

- $|\gamma N\rangle \to |\phi\,(\vec{k}),\ N(-\vec{k}, s_z'^N)\rangle$,
- $|\gamma N\rangle \to |\phi\, N; k, J, J_z, L\rangle$,
- $|\gamma N\rangle \to |\phi\, N; k, J, J_z, \lambda_N'\rangle$,

$k_x, k_y, k_z, s_z'^N$
$k,\ \ J,\ \ J_z,\ \ L$
$k,\ \ J,\ \ J_z, \lambda_N'$

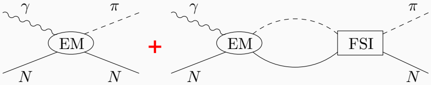

Partial wave decomposition:

$$V_{\alpha,\gamma N}(J,\lambda_N',\lambda_\gamma,\lambda_N;k,q) = 2\pi\int_{-1}^{1}\mathrm{d}(\cos\theta)\sum_{s_z'^N} d^J_{\lambda_\gamma-\lambda_N,-\lambda_N'}(\theta)\,d^{1/2}_{s_z'^N,-\lambda_N'}(\theta)^*\,\mathcal{M}_{\alpha,\gamma N}(s_z'^N,\lambda_N,\lambda_\gamma;\vec{k},\vec{q}),$$

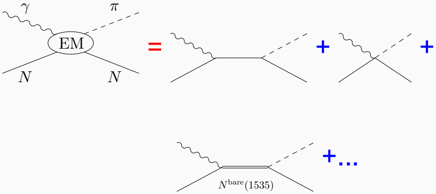

$$V^{JLS;\lambda_\gamma\lambda_N}_{\alpha,\gamma N}(k,q) \quad = \quad \sqrt{\frac{2L+1}{2J+1}}\sum_{\lambda_N'}\langle L,S,0,-\lambda_N'|J,-\lambda_N'\rangle \times V_{\alpha,\gamma N}(J,\lambda_N',\lambda_\gamma,\lambda_N;k,q).$$

D. Guo and Z. W. Liu, Phys. Rev. D **105** (2022) no.11, 11

Electric dipole amplitudes E_{0+} with two bare states

Our results can describe the electric dipole amplitudes E_{0+} extracted from experiments.

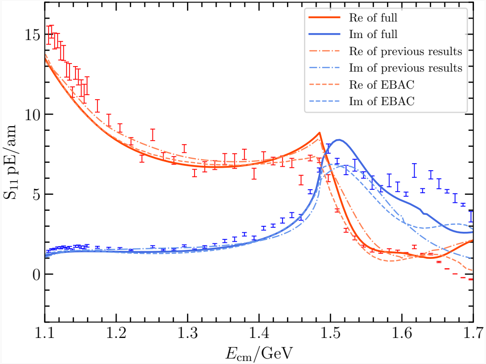

Yu Zhuge, Zhan-Wei Liu, Derek B. Leinweber, Anthony W. Thomas, Phys.Rev.D 110 (2024) 9, 094015.

The bare core in $N^*(1535)$

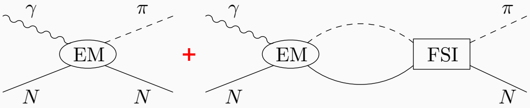

- If $N^*(1535)$ has no bare core, it would play roles ONLY in finite state interaction

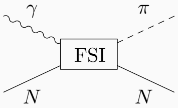

The bare core in $N^*(1535)$

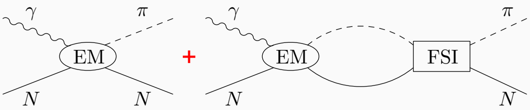

- If $N^*(1535)$ has no bare core, it would play roles ONLY in finite state interaction

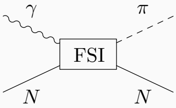

- If with bare core, $N^*(1535)$ also plays roles in electromagnetic potential

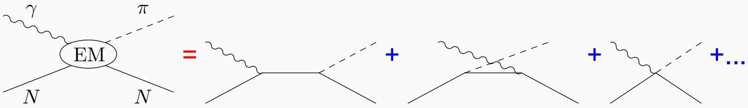

The bare core in $N^*(1535)$

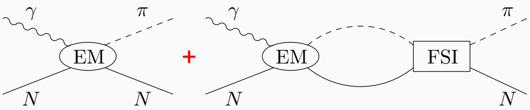

- If $N^*(1535)$ has no bare core, it would play roles ONLY in finite state interaction

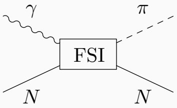

- If with bare core, $N^*(1535)$ also plays roles in electromagnetic potential

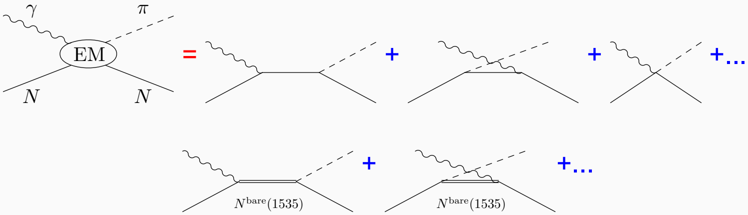

The bare core in $N^*(1535)$ cannot be absent in pion photoproduction

If without the bare core in $N^*(1535)$,
E_0^+ would change much!

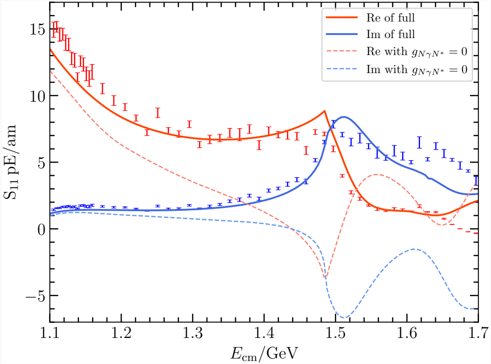

The bare core in $N^*(1535)$ cannot be absent in pion photoproduction

If without the bare core in $N^*(1535)$, E_0^+ would change much!

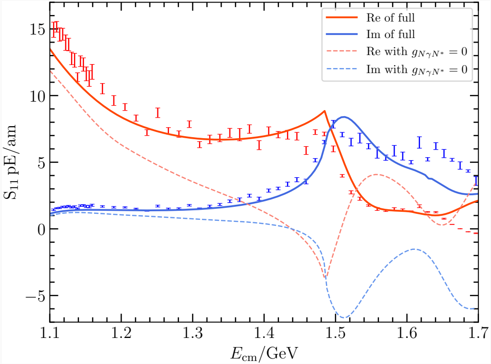

V.S.

If without the bare core in $N^*(1440)$, M_1^- would change little!

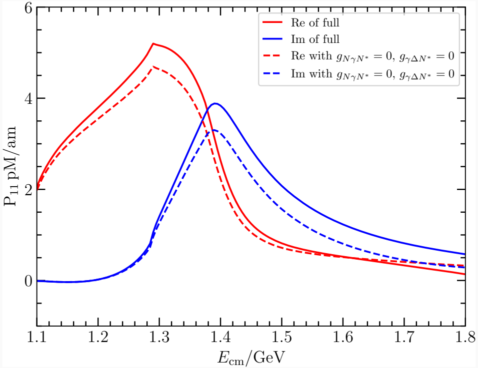

The bare core in $N^*(1535)$ cannot be absent in pion photoproduction

If without the bare core in $N^*(1535)$, E_0^+ would change much!

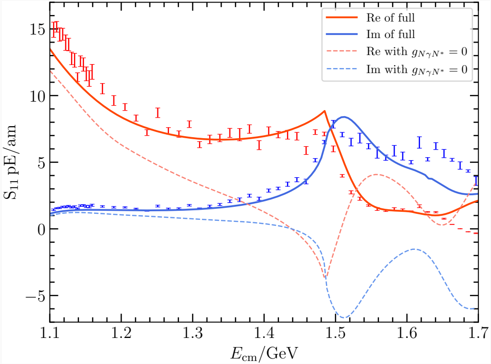

V.S.

If without the bare core in $N^*(1440)$, M_1^- would change little!

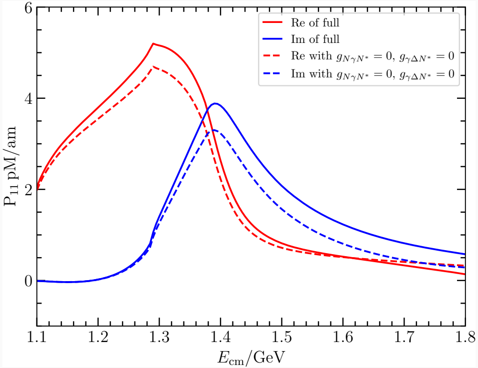

Yu Zhuge, Zhan-Wei Liu, Derek B. Leinweber, Anthony W. Thomas, Phys. Rev. D 110 (2024) 9, 094015.

4. Constraints from the finite-volume $\gamma^* N \to \pi N$

Latest lattice QCD data on E_0^+

The lattice QCD results is very close to the partial wave analysis from the Jülich-Bonn-Washington collaboration.

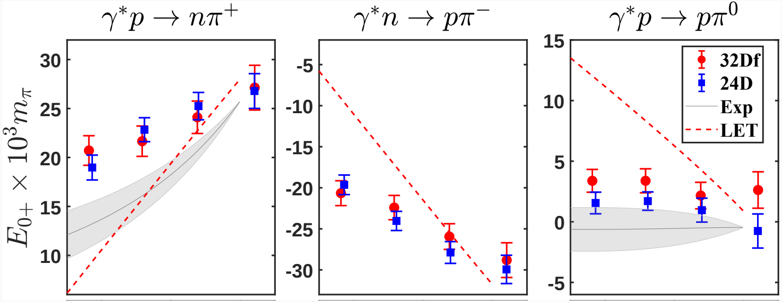

First lattice QCD simulation of pionproduction at threshold!

Gao, Yu-Sheng and Zhang, Zhao-Long and Feng, Xu and Jin, Lu-Chang and Liu, Chuan and Meißner, Ulf-G., Lattice QCD Study of Pion Electroproduction and Weak Production from a Nucleon, Phys. Rev. Lett. 134 (2025) 17, 171904

Direct extension of our previous work

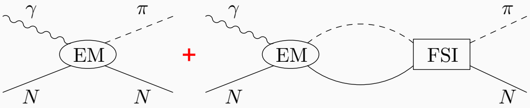

From the real photon ($q^2 = 0$) to the virtual spacelike photon ($q^2 < 0$), we

- do not adjust the previous parameters,
- add the form factors of neutrons and pion:
  - $F(q^2 = 0) = 1$,
  - $F(q^2 < 0) < 1$,
  - $F(q^2)$ is well determined by the experiment.

Latest lattice QCD data and our HEFT results

Our HEFT results can describe the lattice QCD E_{0+} very well.

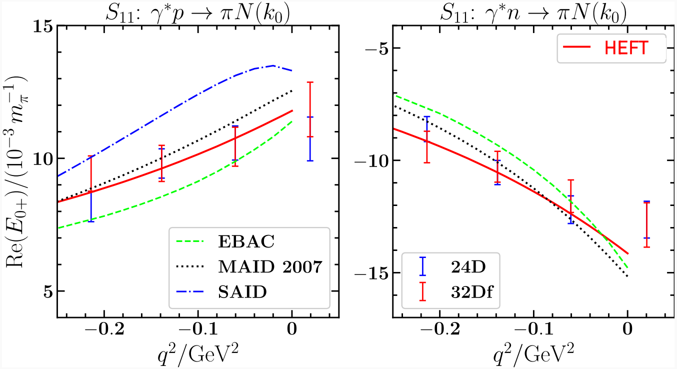

Y. Zhuge, Z.-W. Liu, D. B. Leinweber, A. W. Thomas, arXiv: 2603.06055.

The Lellouch–Lüscher formula

- The original lattice QCD E^{L}_{0+} are not strictly equal to the physical E_{0+}.

- Lellouch & Lüscher proved

  a corrected factor is needed for general electroweak processes *[Lellouch:2000pv]* :

$$F_{\mathrm{LL}} = \left| \frac{E_{0+}|_{E_{G(n)}}}{E^{L}_{0+}|_{E_{G(n)}}} \right| = \sqrt{\frac{2\pi\, C_3(n)}{(kL)^3} \left(\tilde{k}\frac{d\phi}{d\tilde{k}} + k\frac{d\delta}{dk} \right)},$$

where $\tilde{k} \equiv \frac{kL}{2\pi}$, k is πN 3-momentum, $C_3(n)$ represents the number of summing the squares of three integers to equal n.

The function $\phi(\tilde{k})$ is related to the ζ function, and $\delta(k)$ is the phase shift.

- This factor only depends on the final state interactions.

- The published lattice QCD data has been transformed with Lellouch–Lüscher factor.

HEFT can study both infinite volume E_{0+} and finite volume E^L_{0+}

Infinite volume $E_{0+} \sim \quad V_{\pi N,\gamma^* N}(k,q) + \sum_{\alpha=\pi N,\eta N,\dots} \int dk' k'^2 V_{\alpha,\gamma^* N}(k',q) \frac{1}{E_{cm} - \omega_\alpha(k') + i\epsilon} T_{\pi N,\alpha}(k,k';E_{cm})\,,$

Finite volume $E^L_{0+} \sim \quad \sum_{\alpha,n_i} c^{(i)}_{n_i} V_{\alpha(n_i),\gamma * N},$ $\quad c^{(i)}_{n_i}$ is the eigenvector in the box.

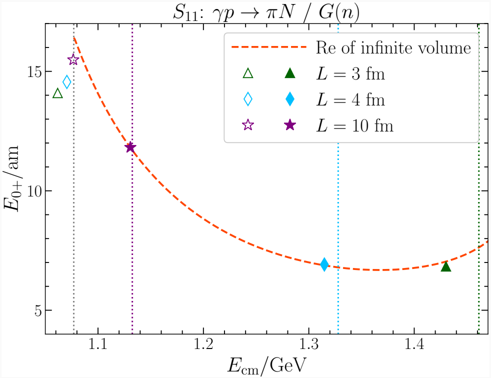

- With L increasing, E^L_{0+} gets closer to E_{0+}.
- The finite volume effects are much smaller for the first excited states compared to the ground states.

Y. Zhuge, Z.-W. Liu, D. B. Leinweber, A. W. Thomas, arXiv: 2603.06055.

We have proposed an extended Lellouch–Lüscher formalism

- The Lellouch–Lüscher formula can only extrapolate the absolute value $|E_{0+}|$

$$F_{\rm LL} = \left| \frac{E_{0+}|_{E_{G(1)}}}{E^L_{0+}|_{E_{G(1)}}} \right| = \sqrt{\frac{12\pi}{(kL)^3} \left(\tilde{k}\frac{d\phi}{d\tilde{k}} + k\frac{d\delta}{dk} \right)} \, .$$

- If separable potentials $V_{\alpha,\alpha'}(k,k') = h_\alpha(k)\, h_{\alpha'}(k')$ are employed, $\alpha^{(\prime)} = \gamma N, \pi N, \eta N, \ldots$,

$$F_{\rm sep} = \frac{E_{0+}|_{E_{G(1)}}}{E^L_{0+}|_{E_{G(1)}}} = \frac{2\sqrt{6}\pi^2\, T_{\pi N,\pi N}\left(E_{G(1)}, k_{G(1)}, k_1\right)}{L^3 U_1^{\rm bind} c_1^{\pi N}} \, ,$$

where $c_1^{\pi N} = \langle \pi N(k_1)|G(1)\rangle = 1 + O(L^{-6}) \approx 1$, $U_1^{\rm bind} = E_{\pi N(1)} - E_{G(1)}$ denotes its finite-volume binding energy and $T_{\pi N,\pi N}$ is corresponding T matrix in infinite volume.

- This simple factor also depends only on the final state interactions.
- It can provide extrapolations to both the real and imaginary parts.

Comparison between Lellouch–Lüscher factor and our extended one

For the first excited state:

		our extended factor			Lellouch–Lüscher factor	
L/fm	$\text{Re}F_{\text{HEFT}}$	$\text{Re}F_{\text{sep}}$	$\text{Im}F_{\text{HEFT}}$	$\text{Im}F_{\text{sep}}$	$\lvert F_{\text{HEFT}}\rvert$	F_{LL}
3	1.029	1.028	0.376	0.375	1.096	1.095
4	0.995	0.990	0.222	0.221	1.019	1.016
10	0.999	0.999	0.122	0.122	1.007	1.006

- The final expression for F_{sep} does not rely on the details in the separable potentials;
- It may be still appropriate even if more complicated potentials are used;
- For example, the Table shows the consistency between F_{sep} and F_{HEFT}.

Both factors are leading approximations for ground states below threshold

In 3 fm box, the ground state of the $1/2^-$ N^* is predominantly πN (more than 99%), with the binding energy $U_0^{\text{bind}} = 15$ MeV below threshold.

- This brings the Lellouch–Lüscher factor one obvious problem: the phaseshifts $\delta(k)$ are not well defined.

$$F_{\text{LL}} = \sqrt{\frac{2\pi}{(kL)^3}\left(\tilde{k}\frac{d\phi}{d\tilde{k}} + k\frac{d\delta}{dk}\right)}\,.$$

Usually one can analytically extends to the unphysical region (eg. using Taylor expansion).

- If using the separable potential approximation

$$F_{\text{sep}} \approx \frac{2\pi a_{\pi N}}{\mu_{\pi N} U_0^{\text{bind}} L^3}\,.$$

- Both factors gives the same results at $O(L^{-1})$ but different at higher orders for eigenstates below threshold

$$F_{\text{sep}/\text{LL}} = 1 + \frac{Z_{00}(1,0)}{\pi}\frac{a_{\pi N}}{L} + O(L^{-2})\,.$$

Both factors are leading approximations for ground states below threshold

- We can numerically show
  this factor depends on both strong and electromagnetic interactions for the ground states

$$F_{\text{HEFT}}\big|_{3\text{fm}}^{\text{Full EM potential}} = 1.164 \qquad vs. \qquad F_{\text{HEFT}}\big|_{3\text{fm}}^{\text{only-contact EM potential}} = 1.209$$

- These two approximations provide estimates at roughly the $O(L^{-1})$ level

$$F_{\text{sep}}\big|_{3\text{fm}} = 1.145 \qquad vs. \qquad F_{\text{LL}}\big|_{3\text{fm}} = 1.206$$

  whose difference can be applied to assess the associated uncertainty.
- Achieving higher accuracy requires a detailed dynamical model incorporating realistic electromagnetic and strong interactions such as HEFT.

Summary

Summary

- We have analyzed
  - (1) $\pi N \to \pi N$
  - (2) lattice QCD spectrum of N^*
  - (3) $\gamma + N \to \pi + N$
  - (4) lattice QCD simulation of pionproduction

- We have proposed a novel extension of the well-known Lellouch-Lüscher formalism that extrapolates both real and imaginary parts of amplitudes for general electroweak processes.

Thank you for your attention!